

Precoded Universal MIMO Superposition Transmission for Achieving Optimal Coverage and High Throughput in 6G and Beyond Networks

Sadiq Iqbal*, Jehad M. HAMAMREH

Abstract—A wireless network can utilize its entire resources to serve users without any allocation and provide upgraded performances such as enhanced throughput and high reliability without interference among users. However, previous wireless communication technologies could not bring the full utilization of network resources and overcome the challenge of forgoing scheduling among users. Therefore, to address these requirements, we propose and develop a novel design coined as Precoded Universal MIMO Superposition Transmission (PU-MIMO-ST) that can also be applicable for the most challenging and worst case interference scenario where the number of antenna points (APs) and the number of user equipment (UEs) is equal. In the considered system model, the APs are linked to a central processing unit (CPU) via backhaul and the UEs receive co-operation from the network resulting in achieving the optimal usage of network resources. The results obtained from computer simulations proof and verify the effectiveness of the proposed design called PU-MIMO-ST compared with other competitive works in terms of reliability, throughput, reduced complexity on the reception side, as well as power conservation.

Index Terms—Multi-user MIMO, massive MIMO, network MIMO, distributed MIMO, distributed antenna system, cell-free massive MIMO, pCell, 6G and Beyond.

I. INTRODUCTION

TO fulfill the communication needs of humans as well as intelligent machines, 6G and beyond networks will be the fundamental components for all parts of life, society, and industry. These networks will pave the way towards realizing the technological aspirations that include holographic telepresence, e-Health, ubiquitous connectivity in smart environments, massive robotics, three-dimensional massive unmanned mobility, augmented reality, virtual reality, and internet of everything [1]. To provide these applications with an effective and efficient wireless communication network than ever with an unparalleled increase in the data rates, massive connectivity, high-reliability, and low latency, 6G and beyond networks will implement promising technologies with different paradigms relevant to massive multiple input multiple output (MMIMO) networks such as network MIMO

(netMIMO), distributed MIMO (D-MIMO), multi-cell MIMO (MC-MIMO), distributed input distributed output (DIDO) and joint transmission coordinated multi-point (JT-CoMP) [1]. The conventional manifestation of the MMIMO system is the collocated MMIMO (C-MMIMO) in which a minority of users are served through a considerable majority of antennas via beamforming. The antennas are located at the base stations (BSs) and share the same temporal-frequency resources [2].

C-MMIMO systems can provide significantly high data rates, high link reliability, coverage, and energy efficiency [3], but suffer from performance degradation for cell-edge users located at cell edges due to the lower channel gain from the serving cell as well as the inter-cell interference. However, unlike the C-MMIMO system, the MMIMO operation can be employed in a distributed mode by arranging the majority of single antenna access points with a central processing unit (CPU). The CPU and access points are linked through a backhaul [4] and the setup is identical to a distributed antenna system (DAS) [5]. Distributed MMIMO (D-MMIMO) systems provide superior data rates than C-MMIMO due to the high diversity gain to each user and good quality-of-service (QoS) to cell-edge users as an outcome of having more APs on the edge users proximity.

A. Relevant D-MMIMO technologies

This subsection is dedicated to briefly overview and talk about the D-MMIMO related technologies like netMIMO, D-MIMO, MC-MIMO, DIDO, and JT-CoMP.

netMIMO: netMIMO can mitigate inter-cell interference (ICI) by synchronizing the access points and sharing data packets. The access points can transmit concurrently to increase the downlink range. A reference signal is utilized to synchronize the access points at the level of the carrier signal, and data is shared among the access points through a wired backhaul [6], [7], [8], [9], [10].

D-MIMO: A generalized DAS, also known as distributed MIMO (D-MIMO), contains the features of point-to-point MIMO and DAS while also achieving enhanced spatial diversity. Besides C-MIMO, the D-MIMO system suffers from path loss due to different distances from discretely scattered antennas, resulting in increasing difficulty of spectral efficiency analysis [11], [12].

MC-MIMO: Wyner presented a multi-cell system with inter-cell cooperation [13], where BSs with multiple antennas can form wireless networks around each other and each cell

Sadiq Iqbal* is with the WISLAB, Department of Electrical Computer Engineering, Antalya Bilim University, Antalya, 07190, Turkey (e-mail: sadiq.zahid73@gmail.com).

* Corresponding Author

Jehad M. HAMAMREH is with the WISLAB, Department of Electrical Electronics Engineering, Antalya Bilim University, Antalya, 07190, Turkey (e-mail: jehad.hamamreh@gmail.com).

Manuscript received Sep 20, 2022; accepted Dec 14, 2022.
DOI: 10.17694/bajece.1177534

All the codes used can be found at researcherstore.com

contains within its range a single-antenna user equipment (UE).

DIDO: DIDO network consists of access points and remote radio units (RRHs), which are utilized in human-type and machine-type communications (MTC) systems. The RRHs are relatively much nearer to UEs [14].

JT-CoMP: JT-CoMP consists of CoMP clusters that have distinct coordinating nodes that broadcast data to a UE consistently or non consistently, and phase information is utilized so that the network can remove inter-user interference [15], [16], [17], [18].

B. CF-MMIMO technologies

Recently, an updated practical version of the D-MMIMO system has emerged and named as cell-free MMIMO (CF-MMIMO) system. This system consists of a CPU connected to all the access points, operating them as an MMIMO network with no cell boundaries. By employing spatial multiplexing, the users are served over the same resources [1]. Even compared with the small-cell (SC) system, the CF-MMIMO system outperforms the fully distributed SC system in terms of the 95% likely per user throughput [19]. In the literature so far, there are many works done on the CF-MMIMO system such as, in [20], authors derive a closed-form expression, and through this expression, an optimal max-min power control scheme can be obtained which provides equivalent quality of service to all users.

Authors in [21] propose a new configuration for scalable CF-MMIMO systems by exploiting the dynamic cooperation cluster concept of netMIMO to scale joint initial access, allotment of pilots with the formation of clusters while having a duality of the uplink and downlink. Concerning the precoding and power optimization in CF-MMIMO, the authors in [22] propose a near-optimal power control algorithm that is considerably simpler than exact max-min power control. Allotment of power method discussed in [23] can increase the energy efficiency, and the authors also developed an access point selection method so that users can select access point subsets that reduce the backhaul link power consumption [23]. In [24], authors present an analysis of CF-MMIMO under distinct degrees of cooperation among the access points and the uplink spectral efficiencies of four different cell-free implementations, with spatially correlated fading and arbitrary linear processing.

Scalability aspects of CF-MMIMO have been investigated in [25]. In this study, the authors proposed a solution related to data processing, network topology, and power control. This framework achieves full scalability at the cost of a meager performance loss compared to the standard form of CF-MMIMO. In [26], authors assume how much downlink pilot can improve the performance of CF-MMIMO and determine that by exploiting downlink pilots in less dense networks, the enhancement in performance can be obtained while staying moderate in a high-density area.

Authors in [27] propose a beyond cell-free MIMO (CF-MMIMO) approach to surround the BSs and users with reconfigurable intelligent surfaces (RISs). In this less costly way,

reconfigurable reflections can produce spreading conditions, thus enhancing CF-MMIMO communication. The study [28] takes a new look at CF-MMIMO via the lens of the dynamic cooperation cluster framework from netMIMO while providing distributed algorithms for merging, initial access, precoding, cluster formation, and assignment of pilots to make them expandable for multiple users.

Another important commercialized application relevant to CF-MMIMO but better in terms of spectral efficiency and presented under the umbrella of the Artemis network is pCell [29] pCell is all about procuring SE multiple times of any other technology by distributing both the transmitters and receivers. The transmitters are scattered while the receivers are packed in a small space. Taking advantage of the interference, coordination between access points and UEs, and equipped with peak spatially multiplexed yields acquired through numerous transmissions. SE gains are reaped without any concept of existing cells [29]. Authors in [29] also consider a unique geometrical spreading channel model that is customized as a merger of plane waves which is different from the one utilized in [19].

So far, we have concisely discussed MMIMO with its relevant distributed technologies, and then we talked about the CF-MMIMO with its technical literature review and the pCell. Given below are the demerits of D-MMIMO and CF-MMIMO that highlight their drawbacks, and then we bring forth our proposed model's advantages that remedy these drawbacks.

C. Shortcomings of D-MMIMO

- 1) D-MMIMO utilize non-cell free approach that makes it harder to achieve total coverage and geographical area flexibility.
- 2) To eliminate ICI, synchronization is needed among access points which increases network's complexity.
- 3) Due to multi-cell scenario, users at the cell edges experience severe degradation in performances and throughput.
- 4) Due to fixed inter-cell cooperation, the resources of the network are divided among users.

D. Shortcomings of CF-MMIMO

- 1) There are no cells present in CF-MMIMO with access points scattered around the perceivable serving area. The number of access points, however, are much larger than the users, leading to uneven sharing of network resources among users.
- 2) Needs scheduling to accommodate users utilizing the resources.
- 3) Super positioning of user data not implemented in CF-MMIMO.

As can be noticed, the aforementioned state-of-the-art technologies do not provide capacity usage of the system with unprecedented spectral efficiency, highest reliability, and interference-free communication to each UE at the same time. These challenges need to be addressed for the future 6G and beyond networks. To meet these requirements and fulfill the shortcomings of the D-MMIMO and CF-MMIMO, in this work, we propose a new novel communication technique.

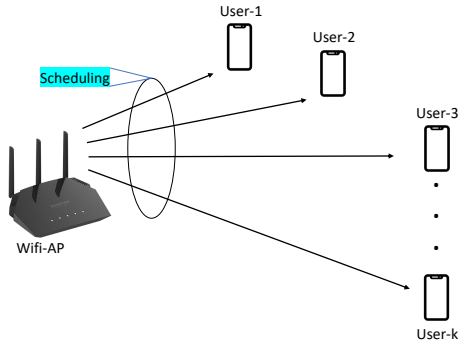


Fig. 1. Representation of a conventional WiFi access points serving multiple users.

E. Contributions of the proposed design

The contributions provided by the proposed design in this work are summarized below:

- 1) The proposed work can directly serve each user with all the resources of a cell in a network which includes several antennas, time slots, spectrum bandwidth, etc., without causing any interference at all.
- 2) The number of APs is made equal to the number of UEs, which results in dedicating the capacity of the network to every UE simultaneously.
- 3) The method is enabled by superimposing the users' data in a very unique and special way to eliminate multiuser interference.
- 4) Specially designed diagonal matrices are utilized along with novel precoding and auxiliary signals that are a function of both user data and the channel effects.

F. Differences & impact of the proposed method

To explain the differences between the proposed design and the state-of-the-art techniques, we consider an example of a WiFi access point as shown in Fig. 1. The access point is installed in a room to initially serve just a single user, who is assumed to be served with a data rate of 50 Mbps for instance. However, when a new user gets connected to the same WiFi access point, the system now communicates with two users and splits the resources and thus the data rate in half so that both users can get 25 Mbps each. The WiFi will split the data according to the number of users associated with it. The WiFi does the splitting of resources in the time domain due to the WiFi spectrum being overly crowded and full of interference.

Scheduling is the same concerning 4G and 5G technologies, but compared with WiFi is much better because cellular systems utilize time and frequency to assign time slots and carriers to a user based on their conditions and service requirements such as text, voice, gaming, video streaming, etc. In scheduling, the process of adjusting, adapting, fixing, redistributing, and reallocating the resources continues to happen as long as there are users trying to get access simultaneously. Therefore, in wireless systems, gaining full optimal capacity is the best-case scenario, which results in allocating the full bandwidth of the access point, BS, or the

tower to every user in the whole network without sharing and with no interference at the user location. One of the main contributions of the proposed design is exactly that as the users number increases, they get the full bandwidth with no splitting or sharing of resources with other users. This makes the proposed design clearly different from CF-MMIMO [19] and pCell [29].

The rest of the paper is structured as follows. Section II expounds the considered system model framework, the channel representation, the proposed theorem that incorporates the introduced superposition concept, and derives the closed-form expressions of the superimposed auxiliary signals and precoding matrices. Section III highlights the performance inspection and measures of the proposed design. Section IV illustrates the simulation results and explains them. Finally, Section V presents the conclusion of the paper¹.

II. SYSTEM LAYOUT

The layout of the proposed system is as shown in Fig. 2, where we consider the number of UEs denoted by K equal to the number of APs signified by M . The APs are connected to a CPU via a backhaul, and both users and access points are placed irregularly in a geographical cell-reprieved environment as shown in Fig. 2, which depicts the general illustration of the proposed scheme comprising three different scenarios ranging from two UEs case to K UEs case and number of K UEs is equal to number of M APs.

A. Transmission

The APs simultaneously transmit to all UEs for achieving the spatial multiplexing property. The data of all UEs are precoded, superimposed on top of each other, and then the auxiliary signals are added to them. After this, the Inverse Fast Fourier Transform (IFFT) is applied to the signals to be transmitted.

B. Channel composition

The complex channel coefficient is styled as the superimposition of plane waves across AP antenna $m=1, \dots, M$ and UE antenna $k=1, \dots, K$

$$h_{km} = \sum_{p \in S_{km}} d_p e^{-i w \hat{v}_p \cdot r_k} \quad (1)$$

In Eq. (1), every path is included in the set S_{km} , such as propagation and cluster scattering through AP antenna m to UE antenna k . Wavenumber $w = 2\pi/\lambda$, λ denotes the wavelength. As shown in Fig. 4, the placement vector of UE k is r_k relative to an origin O , while the unit vector is \hat{v}_p which is in the direction of the incident path p which points out from the position of UE k . d_p on the other hand, is the complex coefficient with specifically designed path loss, shadowing, and phase terms that are unassociated to r_k for path p .

¹Notations: Vectors are expressed and denoted by bold-small letters, whereas matrices are expressed by bold-large letters. The transpose, conjugate transpose, and inverse are symbolized by $(\cdot)^T$, $(\cdot)^H$ and $(\cdot)^{-1}$, respectively. I is the $N \times N$ identity matrix and O is the $N \times N$ Zero matrix.

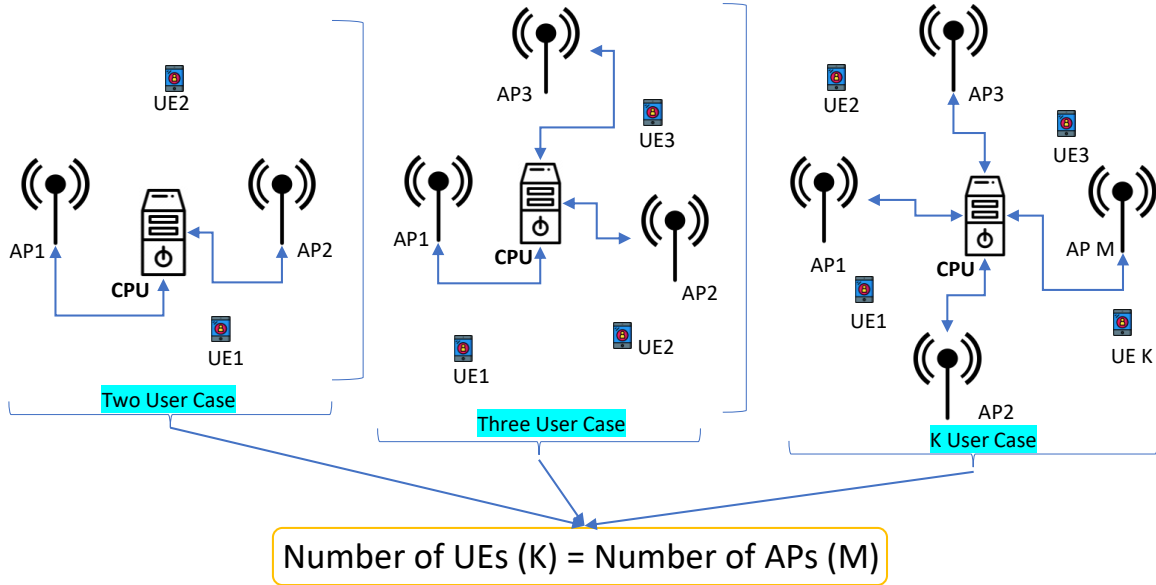


Fig. 2. General system model of the proposed method.

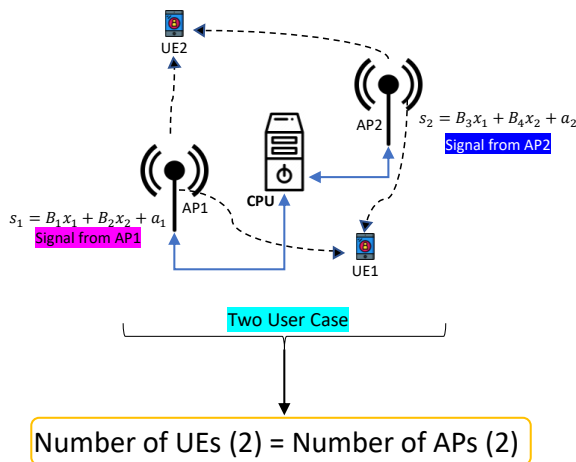


Fig. 3. System model of the proposed method with two access points and two users.

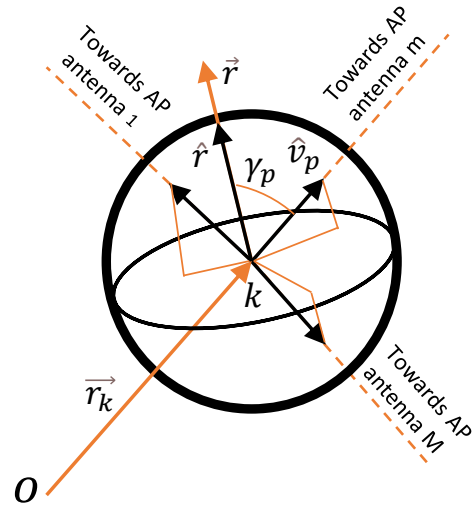


Fig. 4. Design parameters of the channels with angle $\gamma_p \in [0, \pi]$ across directional path \hat{v}_p and direction of displacement \hat{r} .

If we exclude d_p path loss from Eq. 1, we are left with the exponent component, which houses the small scale fading. The average SNR consists of the path loss effect that is received by the UE and the remaining channel components boil down to a Rayleigh fading phenomenon as in [30], [31], [32].

C. Reception

As illustrated in Fig. 3, each of the AP_m and UE_k has a single antenna. The channel matrix detailing the propagation between the transceiver antennas is denoted by H_{km} . The total number of modulated symbols in one OFDM block at each AP for each UE is N_f , thus the frequency response of every OFDM block for each UE is given by

$\mathbf{x}_k = [x_0, x_1, \dots, x_{N_f-1}] \in C^{[N_f \times 1]}$. The auxiliary signal [33] is denoted by \mathbf{a}_q , $q = m$ and precoding matrix [34] indicated by \mathbf{B}_t , $t = 1^2, 2^2, \dots, k^2$ both of which are based on the wireless channel propagation properties. The three case studies will be discussed and the corresponding conditions are illustrated that can be used to find the values of precoders and auxiliary signals.

1) *In case of UE_k with $k = 1, 2$:* As we have presumed earlier $UE_k = AP_m$, AP_1 and AP_2 concurrently transmit the intended superimposed signals s_1 and s_2 to UE_1 and UE_2 . The superimposed signals are as follows:

$$s_1 = \mathbf{B}_1\mathbf{x}_1 + \mathbf{B}_2\mathbf{x}_2 + \mathbf{a}_1, \tag{2}$$

$$\mathbf{s}_2 = \mathbf{B}_3\mathbf{x}_1 + \mathbf{B}_4\mathbf{x}_2 + \mathbf{a}_2, \quad (3)$$

where $\mathbf{B}_1, \mathbf{B}_2, \mathbf{B}_3$ and \mathbf{B}_4 are precoding matrices, while \mathbf{a}_1 and \mathbf{a}_2 are the superimposed auxiliary signals as shown in (2) and (3).

Signals received at \mathbf{UE}_1 :

$$\mathbf{y}_{11} = \mathbf{H}_{11}\mathbf{s}_1, \quad (4)$$

$$\mathbf{y}_{12} = \mathbf{H}_{12}\mathbf{s}_2, \quad (5)$$

$$\hat{\mathbf{y}}_{r_1} = \mathbf{y}_{11} + \mathbf{y}_{12} + \mathbf{z}_1, \quad (6)$$

$$\hat{\mathbf{y}}_{r_1} = \mathbf{H}_{11}\mathbf{s}_1 + \mathbf{H}_{12}\mathbf{s}_2 + \mathbf{z}_1, \quad (7)$$

$$\hat{\mathbf{y}}_{r_1} = \mathbf{H}_{11}(\mathbf{B}_1\mathbf{x}_1 + \mathbf{B}_2\mathbf{x}_2 + \mathbf{a}_1) + \mathbf{H}_{12}(\mathbf{B}_3\mathbf{x}_1 + \mathbf{B}_4\mathbf{x}_2 + \mathbf{a}_2) + \mathbf{z}_1, \quad (8)$$

$$\hat{\mathbf{y}}_{r_1} = (\mathbf{B}_1\mathbf{H}_{11} + \mathbf{B}_3\mathbf{H}_{12})\mathbf{x}_1 + (\mathbf{B}_2\mathbf{H}_{11} + \mathbf{B}_4\mathbf{H}_{12})\mathbf{x}_2 + \mathbf{H}_{11}\mathbf{a}_1 + \mathbf{H}_{12}\mathbf{a}_2 + \mathbf{z}_1. \quad (9)$$

where \mathbf{y}_{11} and \mathbf{y}_{12} are the intended signals for \mathbf{UE}_1 , $\hat{\mathbf{y}}_{r_1}$ is the combined received signal at \mathbf{UE}_1 . \mathbf{H}_{11} and \mathbf{H}_{12} are the channel impulse responses between \mathbf{UE}_1 and both \mathbf{AP}_1 and \mathbf{AP}_2 , while \mathbf{z}_1 is the additive white Gaussian noise present at \mathbf{UE}_1 antenna.

Signals received at \mathbf{UE}_2 :

$$\mathbf{y}_{21} = \mathbf{H}_{21}\mathbf{s}_1, \quad (10)$$

$$\mathbf{y}_{22} = \mathbf{H}_{22}\mathbf{s}_2, \quad (11)$$

$$\hat{\mathbf{y}}_{r_2} = \mathbf{y}_{21} + \mathbf{y}_{22} + \mathbf{z}_2, \quad (12)$$

$$\hat{\mathbf{y}}_{r_2} = \mathbf{H}_{21}\mathbf{s}_1 + \mathbf{H}_{22}\mathbf{s}_2 + \mathbf{z}_2, \quad (13)$$

$$\hat{\mathbf{y}}_{r_2} = \mathbf{H}_{21}(\mathbf{B}_1\mathbf{x}_1 + \mathbf{B}_2\mathbf{x}_2 + \mathbf{a}_1) + \mathbf{H}_{22}(\mathbf{B}_3\mathbf{x}_1 + \mathbf{B}_4\mathbf{x}_2 + \mathbf{a}_2) + \mathbf{z}_2, \quad (14)$$

$$\hat{\mathbf{y}}_{r_2} = (\mathbf{B}_1\mathbf{H}_{21} + \mathbf{B}_3\mathbf{H}_{22})\mathbf{x}_1 + (\mathbf{B}_2\mathbf{H}_{21} + \mathbf{B}_4\mathbf{H}_{22})\mathbf{x}_2 + \mathbf{H}_{21}\mathbf{a}_1 + \mathbf{H}_{22}\mathbf{a}_2 + \mathbf{z}_2. \quad (15)$$

where \mathbf{y}_{21} and \mathbf{y}_{22} are the intended signals for \mathbf{UE}_2 , $\hat{\mathbf{y}}_{r_2}$ is the combined received signal at \mathbf{UE}_2 . \mathbf{H}_{21} and \mathbf{H}_{22} are the channel impulse responses between \mathbf{UE}_2 and both \mathbf{AP}_1 and \mathbf{AP}_2 , while \mathbf{z}_2 is the additive white Gaussian noise available at \mathbf{UE}_2 antenna.

2) In case of \mathbf{UE}_k and \mathbf{AP}_m : The generalized closed form expressions of the transmitted and received signals are as follows.

$$\mathbf{s}_m = \sum_{k=1}^K \mathbf{B}_t\mathbf{x}_k + \mathbf{a}_q, \quad (16)$$

$$\hat{\mathbf{y}}_{r_k} = \sum_{m=1}^M \mathbf{H}_{km}\mathbf{s}_m + \mathbf{z}_k. \quad (17)$$

Eqs. (16) and (17) represent the transmitted \mathbf{s}_m and received $\hat{\mathbf{y}}_{r_k}$ signals for the k_{th} user. In Eq. (16), the \mathbf{B}_t is the designed precoder, \mathbf{x}_k denotes the user data of the k_{th} user, and \mathbf{a}_q is the auxiliary signal. Eq. (17) includes \mathbf{H}_{km} , \mathbf{s}_m and \mathbf{z}_k that are the channel impulse response between the k_{th} user and m_{th} \mathbf{AP} , m_{th} signal and the additive white Gaussian noise at the k_{th} \mathbf{UE} .

3) Designing the conditional system of equations for precoders and auxiliary signals: For a user (\mathbf{UE}_k) to receive its data, the interference from other \mathbf{UE}_s and the channel effects on this user must be removed. This outcome can be obtained by the system of equations given below.

In the case of two users, the precoding conditions for each user are to equate the required data expression to the identity matrix and the unwanted terms to the null matrix. From Eq. (9), the term associated with \mathbf{x}_1 is equated to the identity matrix and the term linked to \mathbf{x}_2 is equated to a null matrix such as:

$$\mathbf{B}_1\mathbf{H}_{11} + \mathbf{B}_3\mathbf{H}_{12} = \mathbf{I}, \quad (18)$$

$$\mathbf{B}_2\mathbf{H}_{11} + \mathbf{B}_4\mathbf{H}_{12} = \mathbf{O}, \quad (19)$$

From Eq. (15), the term multiplying \mathbf{x}_1 is equated to the null matrix and the expression multiplying \mathbf{x}_2 is equated to an identity matrix like:

$$\mathbf{B}_1\mathbf{H}_{21} + \mathbf{B}_3\mathbf{H}_{22} = \mathbf{O}, \quad (20)$$

$$\mathbf{B}_2\mathbf{H}_{21} + \mathbf{B}_4\mathbf{H}_{22} = \mathbf{I}, \quad (21)$$

Therefore, by following Eqs. (18), (19), (20), and (21), the conditions for deriving the precoders for two users with $k = 1, 2$ can be written. Eqs. (18) and (20) can be combined to form a system of equations (22) and by solving this system the values of precoders \mathbf{B}_1 and \mathbf{B}_3 can be determined.

$$\begin{cases} \mathbf{B}_1\mathbf{H}_{11} + \mathbf{B}_3\mathbf{H}_{12} = \mathbf{I}, \\ \mathbf{B}_1\mathbf{H}_{21} + \mathbf{B}_3\mathbf{H}_{22} = \mathbf{O}, \end{cases} \quad (22)$$

Similar to Eqs. (18) and (20), by combining Eqs. (21) and (19) to form a system of equations (23), the values of precoders \mathbf{B}_2 and \mathbf{B}_4 can be calculated.

$$\begin{cases} \mathbf{B}_2\mathbf{H}_{21} + \mathbf{B}_4\mathbf{H}_{22} = \mathbf{I}, \\ \mathbf{B}_2\mathbf{H}_{11} + \mathbf{B}_4\mathbf{H}_{12} = \mathbf{O}. \end{cases} \quad (23)$$

The above precoder conditions illustrate systems of equations that represent the pattern of increase in equations in the system and the increase of the system as a whole. For $k = 1, 2$, there are two systems of equations with a pair of equations

in each system, this leads to a generalization of the system of equations for k_{th} user such as:

$$n = 2, 3, \dots, N \rightarrow \begin{cases} \sum_{m=1}^M \mathbf{B}_t \mathbf{H}_{km} \mathbf{x}_k = \mathbf{I}, \\ \sum_{m=1}^M \mathbf{B}_t \mathbf{H}_{km} = \mathbf{O}. \end{cases} \quad (24)$$

where $n = 2, 3, \dots, N$ is the increase in number of equations inside the system of equations starting from two and $N \equiv k_{th}$ user.

Now the conditional system of equations for auxiliary signals will be derived for two users with $k = 1, 2$. From Eq. (9), for the first user the first term is the required one, the second, third, and fourth terms are equated to the null matrix, like:

$$(\mathbf{B}_2 \mathbf{H}_{11} + \mathbf{B}_4 \mathbf{H}_{12}) \mathbf{x}_2 + \mathbf{H}_{11} \mathbf{a}_1 + \mathbf{H}_{12} \mathbf{a}_2 = \mathbf{O}, \quad (25)$$

From Eq. (15), for the second user, the second term is the desired term, thus the first, third, and fourth terms are equated to the null matrix as shown below:

$$(\mathbf{B}_1 \mathbf{H}_{21} + \mathbf{B}_3 \mathbf{H}_{22}) \mathbf{x}_1 + \mathbf{H}_{21} \mathbf{a}_1 + \mathbf{H}_{22} \mathbf{a}_2 = \mathbf{O}. \quad (26)$$

Now for calculating the auxiliary signals the conditional system of equations can be derived by combining the Eqs. (25) and (26) as:

$$\begin{cases} (\mathbf{B}_2 \mathbf{H}_{11} + \mathbf{B}_4 \mathbf{H}_{12}) \mathbf{x}_2 + \mathbf{H}_{11} \mathbf{a}_1 + \mathbf{H}_{12} \mathbf{a}_2 = \mathbf{O}. \\ (\mathbf{B}_1 \mathbf{H}_{21} + \mathbf{B}_3 \mathbf{H}_{22}) \mathbf{x}_1 + \mathbf{H}_{21} \mathbf{a}_1 + \mathbf{H}_{22} \mathbf{a}_2 = \mathbf{O}. \end{cases} \quad (27)$$

Eq. (27) represents the conditional system of equations for finding the values of auxiliary signals for two users case. By finding these assumptions, we can formalize the general form of a system of equations as follows:

$$n \begin{cases} \sum_{c=n-k}^K ((\sum_{m=1}^M \mathbf{B}_t \mathbf{H}_{km}) \mathbf{x}_k) + \sum_{m=1}^M \mathbf{H}_{km} \mathbf{a}_q = \mathbf{O}, \\ \sum_{c=n-k}^K ((\sum_{m=1}^M \mathbf{B}_t \mathbf{H}_{km}) \mathbf{x}_k) + \sum_{m=1}^M \mathbf{H}_{km} \mathbf{a}_q = \mathbf{O}. \end{cases} \quad (28)$$

The null matrix \mathbf{O} is equated to every equation in the system of equations to fulfill the conditions required for the calculation of auxiliary signals.

Designing precoders for the proposed method:

From Eq. (22) the values of precoders \mathbf{B}_1 and \mathbf{B}_3 can be derived by using the mathematical substitution method.

$$\mathbf{B}_1 = -\mathbf{H}_{22}(\mathbf{H}_{12} \mathbf{H}_{21} - \mathbf{H}_{11} \mathbf{H}_{22})^{-1}, \quad (29)$$

$$\mathbf{B}_3 = \mathbf{H}_{21}(\mathbf{H}_{12} \mathbf{H}_{21} - \mathbf{H}_{11} \mathbf{H}_{22})^{-1}, \quad (30)$$

For precoders \mathbf{B}_2 and \mathbf{B}_4 , the system of equations in (23) can be solved to get the precoder values such as:

$$\mathbf{B}_2 = -\mathbf{H}_{12}(\mathbf{H}_{11} \mathbf{H}_{22} - \mathbf{H}_{12} \mathbf{H}_{21})^{-1}, \quad (31)$$

$$\mathbf{B}_4 = \mathbf{H}_{11}(\mathbf{H}_{11} \mathbf{H}_{22} - \mathbf{H}_{12} \mathbf{H}_{21})^{-1}. \quad (32)$$

Designing auxiliary signals for the proposed method:

For finding the values of auxiliary signals in the case of two UEs, the conditional system of equations such as (27) will

be concurrently solved by substitution method to obtain the required solutions for \mathbf{a}_1 and \mathbf{a}_2 as:

$$\mathbf{a}_2 = (\mathbf{H}_{11}(\mathbf{B}_1 \mathbf{H}_{21} + \mathbf{B}_3 \mathbf{H}_{22}) \mathbf{x}_1 - \mathbf{H}_{21}(\mathbf{B}_2 \mathbf{H}_{11} + \mathbf{B}_4 \mathbf{H}_{12}) \mathbf{x}_2)(\mathbf{H}_{12} \mathbf{H}_{21} - \mathbf{H}_{11} \mathbf{H}_{22})^{-1}, \quad (33)$$

$$\mathbf{a}_1 = (-\mathbf{H}_{22}(\mathbf{B}_1 \mathbf{H}_{21} + \mathbf{B}_3 \mathbf{H}_{22}) \mathbf{x}_1 - \mathbf{H}_{22} \mathbf{a}_2)(\mathbf{H}_{21})^{-1}. \quad (34)$$

III. PERFORMANCE INSPECTION

This section is dedicated to the inspection of the performance analysis of the proposed technique. The proposed method's SNR is the function of the instantaneous power of the effective corresponding channel. Therefore, we are required to calculate the distributions associated with this quantity to find the distribution related to P_{γ_b} .

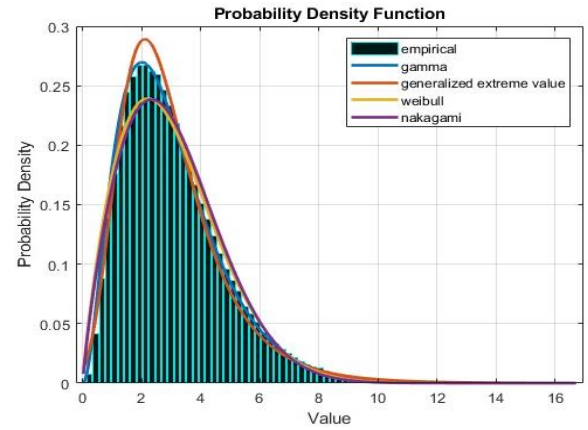


Fig. 5. Amplitude (Power) distribution of the effective fading channel of UE_1 .

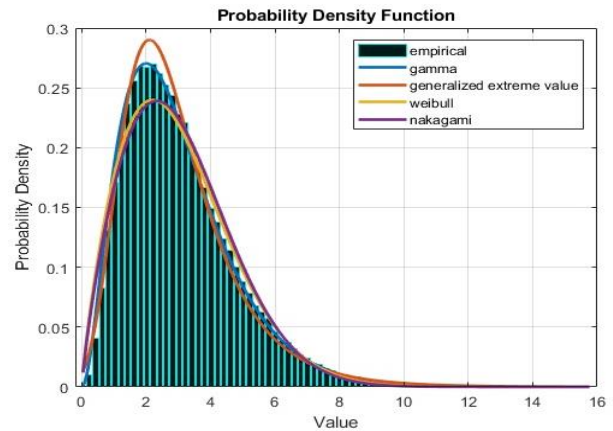


Fig. 6. Amplitude (Power) distribution of the effective fading channel of UE_2 .

A. Bit error rate (BER) analysis

To analyze the BER performance of the proposed scheme, since BPSK is used as a modulation in the scheme, the BER can be expressed in terms of [35] as

$$BER_{UE_k} = \frac{1}{2} \int_0^{\infty} \text{erfc}(\sqrt{\gamma_b}) P_{\gamma_b}(\gamma_b) d\gamma_b \quad (35)$$

where $\text{erfc}(\cdot)$ denotes the complementary error function, $P_{\gamma_b}(\gamma_b)$ is concerned with instantaneous SNR of the appropriate user as well as fading distribution and is termed as probability distribution function (PDF) as in [36].

$$P_{\gamma_b}(\gamma_b) = \frac{P_\alpha(\sqrt{\frac{\Omega\gamma_b}{\bar{\gamma}_b}})}{2\sqrt{\frac{\gamma_b\bar{\gamma}_b}{\Omega}}} \quad (36)$$

In Eq. (36), α denotes the effective channel of the concerned UE. For user 1 the effective channel is shown below:

$$\mathbf{B}_1\mathbf{H}_{11} + \mathbf{B}_3\mathbf{H}_{12}, \quad (37)$$

Similarly, for user 2, the effective is given below:

$$\mathbf{B}_2\mathbf{H}_{21} + \mathbf{B}_4\mathbf{H}_{22}. \quad (38)$$

In Eq. (36), Ω is the mean square of the channel fading amplitude $\Omega = \mathbb{E}\{\alpha^2\}$ while $\bar{\gamma}_b$ is the average SNR. Figs. 5 and 6 illustrate the distributions of effective fading channels of the two users, different distributions are fitted by using data fitting methods. From Figs. 5 and 6, Gamma distribution is the best fit due to the effective channels of the both users with shape and scale parameters a and b . The fading distribution can be described by the following, (D_α).

$$(D_\alpha) \begin{cases} P_\alpha(\alpha) = \frac{1}{b^a\Gamma(a)}\alpha^{(a-1)}\exp(\frac{-\alpha}{b}) \\ (a_1, b_1) = (2.9849, 1.0069) \\ (a_2, b_2) = (2.9876, 1.0035) \end{cases} \quad (39)$$

Eq. (39) represents the expression for the fading profile of the effective channel of one user (denoted by shape and scale parameters a_1 and b_1 and a_2 and b_2), now the effective SNR PDF can be written as:

$$\begin{cases} P_{\gamma_b}(\gamma_b) = G\sqrt{\gamma_b}^{(a-2)}\exp(-(\frac{\sqrt{\Omega}}{b\sqrt{\gamma_b\bar{\gamma}_b}})\gamma_b) \\ G = \frac{1}{2b^a\Gamma(a)}\sqrt{\frac{\Omega^a}{\bar{\gamma}_b^a}} \end{cases} \quad (40)$$

where $\Gamma(\cdot)$ is the gamma function.

To calculate the BER including $\text{erfc}(\cdot)$ for the required user PDF profile, we substitute (40) in the BER $\text{erfc}(\cdot)$ expression (35), then we get the following BER integral form as

$$BER_{\gamma_b} = G\frac{1}{2}\int_0^\infty \text{erfc}(\sqrt{\gamma_b})\sqrt{\gamma_b}^{(a-2)} \exp(-(\frac{\sqrt{\Omega}}{b\sqrt{\gamma_b\bar{\gamma}_b}})\gamma_b), d\gamma_b \quad (41)$$

The integral in Eq. (41) is of the same format presented in [37] and is given as:

$$\int_0^\infty \text{erfc}(\sqrt{x})\sqrt{x}\exp(-\beta x)dx = \frac{1}{2\sqrt{\pi}}\left(\frac{\arctan(\sqrt{\beta})}{(\beta)^{3/2}} - \frac{1}{2\beta(1+\beta)}\right), \beta > 0. \quad (42)$$

In Eq. (42) $\arctan(\cdot)$ denotes the inverse tangent function. To write the BER equation in (41) in the form of this integral by associating $a-2=1$ and appointing

$$\beta = -(\frac{\sqrt{\Omega}}{b\sqrt{\gamma_b\bar{\gamma}_b}})\gamma_b. \quad (43)$$

It is possible to solve the concerning integration which leads to an approximate expression for the BER given as

$$BER_{\gamma_b} \approx \frac{G}{4\sqrt{\pi}}\left(\frac{\arctan(\sqrt{\beta})}{(\beta)^{3/2}} - \frac{1}{2\beta(1+\beta)}\right) \quad (44)$$

Under change of parameters Eq. (44) gives an approximate expression for BER of \mathbf{UE}_1 (and the same for \mathbf{UE}_2).

B. Evaluation of signal to interference plus noise ratio (SINR) for the proposed method

Due to the proposed system model, the interference caused by the data super-position and the channel effects experienced by the concerned user data are removed by the precoder matrices and auxiliary signals. The signals that are received at \mathbf{UE}_1 and \mathbf{UE}_2 expressed by the equations (9) and (15) after removing interference and elimination of channel effects can be further simplified as:

$$\mathbf{y}_{r_1} = \mathbf{x}_1 + \mathbf{z}_1 \quad (45)$$

$$\mathbf{y}_{r_2} = \mathbf{x}_2 + \mathbf{z}_2 \quad (46)$$

Eqs. (45) and (46) give the intended data symbols for the related \mathbf{UE}_s . Now, the following derivations will be related to the SINR for the proposed framework. The metrics imposing for the \mathbf{UE}_1 and \mathbf{UE}_2 's SINRs are as follows:

$$SINR_{\mathbf{UE}_k} = \frac{S_{p_m}}{I_{p_k} + \sigma_z^2} \quad (47)$$

where S_{p_m}, I_{p_k} and σ_z^2 denote the signal power, the interference power and the noise variance for the concerned \mathbf{UE} . SINR for \mathbf{UE}_1 and \mathbf{UE}_2 can be derived from the equations (45) and (46) and written as:

$$SINR_{\mathbf{UE}_1} = \frac{\|\mathbf{I}_1\|^2}{\sigma_{z_1}^2} \quad (48)$$

$$SINR_{\mathbf{UE}_2} = \frac{\|\mathbf{I}_2\|^2}{\sigma_{z_2}^2} \quad (49)$$

where \mathbf{I}_1 and \mathbf{I}_2 denoted the identity matrices.

IV. SIMULATED RESULTS

Simulation results showing the proposed method's performance in terms of BER, throughput error rate (TER), and peak to average power ratio (PAPR) are displayed and discussed in this section. The inspection of the system performance is based on the Rayleigh fading channel model as depicted in Table 1.

In Fig. 7, the BER performances of the proposed design, conventional MIMO systems, and proposed system utilizing auxiliary signals (AS) and precoding (PR) methods independently are presented. The BER performances $BER_1 - (\mathbf{AP} = 2)$ and $BER_2 - (\mathbf{AP} = 2)$ with APs equal to two are higher than MIMO (nTx=2 and nRx=2) with

TABLE I
PARAMETERS UTILIZED.

Type of Modulation	BPSK
IFFT / FFT size	64
Channel model	Rayleigh
Channel delay samples	[0 3 5 6 8]
Channel tap profile (dBm)	[0 -8 -17 -21 -25]
Guard interval length	16
Number of iterations	20000
Symbols per frame	1
Number of bits per second	1
Modulation order	2

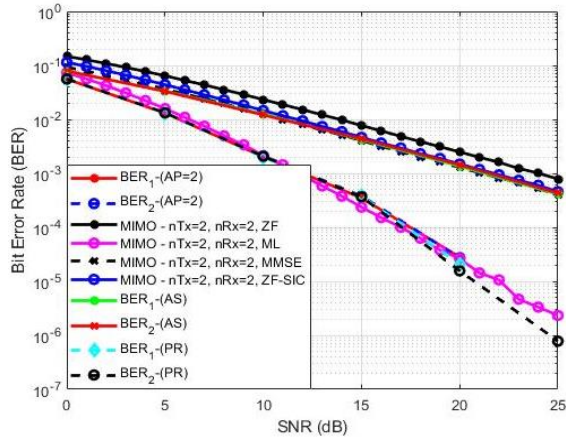


Fig. 7. Bit error rate: Showing the performances of proposed and conventional MIMO systems.

zero-forcing (ZF), maximum likelihood (ML), minimum mean square error (MMSE), and ZF with successive interference cancellation (ZF-SIC) methods. This comparison illustrates the effectiveness of the proposed design.

We can also see the comparison of the illustrations of the BER performances $BER_1 - AS$, $BER_2 - AS$ representing the system using AS superposition method and $BER_1 - PR$, $BER_2 - PR$ representing system utilizing PR method with conventional MIMO systems mentioned above. The AS method has the identical BER performance to ZF, MMSE_i, and ZF-SIC methods but is less than ML. However, due to its unique design, the PR technique has higher BER performance than all the conventional methods. Therefore, the proposed method's BER performance is the culmination of both AS and PR methods evolving into overall higher performance as depicted in Fig. 7.

Fig. 8 illustrates the TER performances of the proposed design $TER_1 - (AP = 2)$, $TER_2 - (AP = 2)$, total $TER - (AP = 2)$, and conventional MIMO ZF, ML, MMSE, and ZF-SIC systems. The proposed scheme has a higher TER than all the MIMO methods portrayed in Fig. 8. The total TER gain result is shown, which is double that of the individual TER_1 , TER_2 , and conventional MIMO TER performances generated by the super-positioned method of the proposed technique.

Moreover, Fig. 9 displays the PAPR gain of the proposed technique compared to the Conv. OFDM, system. The findings show that the proposed design can save power and is less complex than the conventional wireless systems.

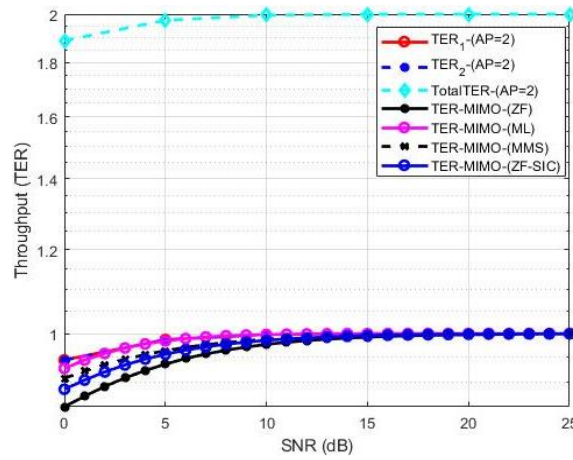


Fig. 8. Throughput error rate: Showing the TER performances for proposed and conventional MIMO systems.

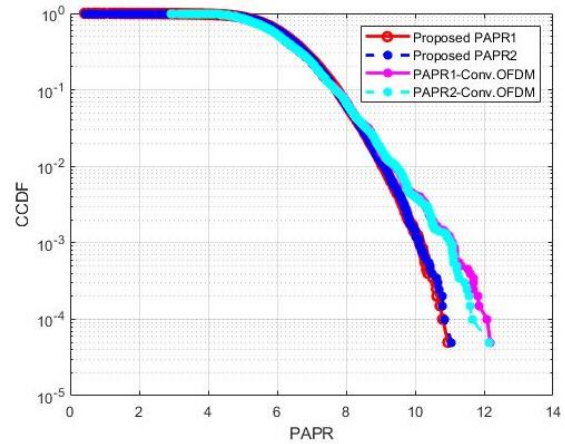


Fig. 9. Peak to Average Power Ratio: Illustrates the performances of proposed model ($PAPR_1$ and $PAPR_2$) and conventional OFDM system.

V. CONCLUSION

In this paper, we introduced and demonstrated a novel transmission scheme called PU-MIMO-ST that allows the optimal full utilization of network resources by each user, thus resulting in achieving high throughput gain thanks to the specially designed method of super-positioning the users data before transmission. The AS and PR matrices cancel the inter-antenna, inter-user interference, and channel effects before reaching the receiver, thus producing outcomes such as less complexity and processing at each UE. The obtained computer simulation results prove that the performance of the proposed system is better than the individual systems utilizing AS, PR, and conventional MIMO based systems. We also intend to extend the proposed technique to existing papers [36], [38], [39], [34], [40], [41], [42], [43], [44], [45], [46], [47], [48], [49], [50], [51], [52] that are related to signal superposition, auxiliary signals, and precoding methods.

REFERENCES

[1] S. Elhoushy, M. Ibrahim, and W. Hamouda, "Cell-free massive MIMO: A survey," *IEEE Communications Surveys & Tutorials*, vol. 24, no. 1, 2021.

- [2] M. A. Albreem, M. Juntti, and S. Shahabuddin, "Massive MIMO detection techniques: A survey," *IEEE Communications Surveys & Tutorials*, vol. 21, no. 4, pp. 3109–3132, 2019.
- [3] N. Fatema, G. Hua, Y. Xiang, D. Peng, and I. Natgunanathan, "Massive MIMO linear precoding: A survey," *IEEE systems journal*, vol. 12, no. 4, pp. 3920–3931, 2017.
- [4] J. Wu, Z. Zhang, Y. Hong, and Y. Wen, "Cloud radio access network (C-RAN): a primer," *IEEE network*, vol. 29, no. 1, pp. 35–41, 2015.
- [5] S. Elhoshy, M. Ibrahim, M. Ashour, T. Elshabrawy, H. Hammad, and M. M. Rizk, "A dimensioning framework for indoor DAS LTE networks," in *2016 International Conference on Selected Topics in Mobile & Wireless Networking (MoWNeT)*. IEEE, 2016, pp. 1–8.
- [6] X. Zhang, K. Sundaresan, M. A. Khojastepour, S. Rangarajan, and K. G. Shin, "NEMOx: Scalable network MIMO for wireless networks," in *Proceedings of the 19th annual international conference on Mobile computing & networking*, 2013, pp. 453–464.
- [7] D. Gesbert, S. Hanly, H. Huang, S. S. Shitz, O. Simeone, and W. Yu, "Multi-cell MIMO cooperative networks: A new look at interference," *IEEE journal on selected areas in communications*, vol. 28, no. 9, pp. 1380–1408, 2010.
- [8] H. V. Balan, R. Rogalin, A. Michaloliakos, K. Psounis, and G. Caire, "Achieving high data rates in a distributed MIMO system," in *Proceedings of the 18th annual international conference on Mobile computing and networking*, 2012, pp. 41–52.
- [9] S. Gollakota, S. D. Perli, and D. Katabi, "Interference alignment and cancellation," in *Proceedings of the ACM SIGCOMM 2009 conference on Data communication*, 2009, pp. 159–170.
- [10] K. C.-J. Lin, S. Gollakota, and D. Katabi, "Random access heterogeneous MIMO networks," *ACM SIGCOMM Computer Communication Review*, vol. 41, no. 4, pp. 146–157, 2011.
- [11] W. Roh and A. Paulraj, "MIMO channel capacity for the distributed antenna," in *Proceedings IEEE 56th Vehicular Technology Conference*, vol. 2. IEEE, 2002, pp. 706–709.
- [12] W. Choi and J. G. Andrews, "Downlink performance and capacity of distributed antenna systems in a multi-cell environment," *IEEE transactions on wireless communications*, vol. 6, no. 1, pp. 69–73, 2007.
- [13] A. D. Wyner, "Shannon-theoretic approach to a Gaussian cellular multiple-access channel," *IEEE Transactions on Information Theory*, vol. 40, no. 6, pp. 1713–1727, 1994.
- [14] J. Choi, "Compressive random access for MTC in distributed input distributed output systems," in *2017 IEEE 85th Vehicular Technology Conference (VTC Spring)*. IEEE, 2017, pp. 1–5.
- [15] A. Davydov, G. Morozov, I. Bolotin, and A. Papathanassiou, "Evaluation of joint transmission CoMP in C-RAN based LTE-A HetNets with large coordination areas," in *2013 IEEE Globecom Workshops (GC Wkshps)*. IEEE, 2013, pp. 801–806.
- [16] A. Barbieri, P. Gaal, S. Geirhofer, T. Ji, D. Malladi, Y. Wei, and F. Xue, "Coordinated downlink multi-point communications in heterogeneous cellular networks," in *2012 Information Theory and Applications Workshop*. IEEE, 2012, pp. 7–16.
- [17] G. Li, S. Zhang, X. Yang, F. Liao, T.-f. Ngai, S. Zhang, and K. Chen, "Architecture of GPP based, scalable, large-scale C-RAN BBU pool," in *2012 IEEE Globecom Workshops*. IEEE, 2012, pp. 267–272.
- [18] B. Clerckx, G. Kim, J. Choi, and Y.-J. Hong, "Explicit vs. implicit feedback for SU and MU-MIMO," in *2010 IEEE Global Telecommunications Conference GLOBECOM 2010*. IEEE, 2010, pp. 1–5.
- [19] H. Q. Ngo, A. Ashikhmin, H. Yang, E. G. Larsson, and T. L. Marzetta, "Cell-free massive MIMO versus small cells," *IEEE Transactions on Wireless Communications*, vol. 16, no. 3, pp. 1834–1850, 2017.
- [20] Ngo, Ashikhmin, Yang, Larsson, and Marzetta, "Cell-free massive MIMO: Uniformly great service for everyone," pp. 201–205, 2015.
- [21] E. Björnson and L. Sanguinetti, "Scalable cell-free massive MIMO systems," *IEEE Transactions on Communications*, vol. 68, no. 7, pp. 4247–4261, 2020.
- [22] E. Nayebi, A. Ashikhmin, T. L. Marzetta, H. Yang, and B. D. Rao, "Precoding and power optimization in cell-free massive MIMO systems," *IEEE Transactions on Wireless Communications*, vol. 16, no. 7, pp. 4445–4459, 2017.
- [23] H. Q. Ngo, L.-N. Tran, T. Q. Duong, M. Matthaiou, and E. G. Larsson, "On the total energy efficiency of cell-free massive MIMO," *IEEE Transactions on Green Communications and Networking*, vol. 2, no. 1, pp. 25–39, 2017.
- [24] E. Björnson and L. Sanguinetti, "Making cell-free massive MIMO competitive with MMSE processing and centralized implementation," *IEEE Transactions on Wireless Communications*, vol. 19, no. 1, pp. 77–90, 2019.
- [25] G. Interdonato, P. Frenger, and E. G. Larsson, "Scalability aspects of cell-free massive MIMO," in *JCC 2019-2019 IEEE International Conference on Communications (ICC)*. IEEE, 2019, pp. 1–6.
- [26] G. Interdonato, H. Q. Ngo, E. G. Larsson, and P. Frenger, "How much do downlink pilots improve cell-free massive MIMO?" in *2016 IEEE Global Communications Conference (GLOBECOM)*. IEEE, 2016, pp. 1–7.
- [27] Y. Zhang, B. Di, H. Zhang, J. Lin, C. Xu, D. Zhang, Y. Li, and L. Song, "Beyond cell-free MIMO: energy efficient reconfigurable intelligent surface aided cell-free MIMO communications," *IEEE Transactions on Cognitive Communications and Networking*, vol. 7, no. 2, pp. 412–426, 2021.
- [28] E. Björnson and L. Sanguinetti, "A new look at cell-free massive MIMO: Making it practical with dynamic cooperation," in *2019 IEEE 30th Annual International Symposium on Personal, Indoor and Mobile Radio Communications (PIMRC)*. IEEE, 2019, pp. 1–6.
- [29] A. Forenza, S. Perlman, F. Saibi, M. Di Dio, R. Van Der Laan, and G. Caire, "Achieving large multiplexing gain in distributed antenna systems via cooperation with pcell technology," in *2015 49th Asilomar Conference on Signals, Systems and Computers*. IEEE, 2015, pp. 286–293.
- [30] J. Qiu, K. Xu, X. Xia, Z. Shen, and W. Xie, "Downlink power optimization for cell-free massive MIMO over spatially correlated Rayleigh fading channels," *IEEE Access*, vol. 8, pp. 56214–56227, 2020.
- [31] J. Qiu, K. Xu, Z. Shen, W. Xie, D. Zhang, and X. Li, "Downlink performance analysis of cell-free massive MIMO over spatially correlated Rayleigh channels," in *2019 IEEE 19th International Conference on Communication Technology (ICCT)*. IEEE, 2019, pp. 122–127.
- [32] G. Interdonato, H. Q. Ngo, E. G. Larsson, and P. Frenger, "On the performance of cell-free massive MIMO with short-term power constraints," in *2016 IEEE 21st International Workshop on Computer Aided Modelling and Design of Communication Links and Networks (CAMAD)*. IEEE, 2016, pp. 225–230.
- [33] J. P. Lemayian and J. M. Hamamreh, "Novel small-scale NOMA communication technique using auxiliary signal superposition," in *2020 International Conference on UK-China Emerging Technologies (UCET)*. IEEE, 2020, pp. 1–4.
- [34] J. Lemayian and J. Hamamreh, "Hybrid MIMO: a new transmission method for simultaneously achieving spatial multiplexing and diversity gains in MIMO systems," *RS Open Journal on Innovative Communication Technologies*, vol. 2, no. 4, 2021.
- [35] J. M. Hamamreh, E. Basar, and H. Arslan, "OFDM-subcarrier index selection for enhancing security and reliability of 5G URLLC services," *IEEE Access*, vol. 5, pp. 25 863–25 875, 2017.
- [36] M. Abewa and J. M. Hamamreh, "Multi-user auxiliary signal superposition transmission (mu-as-st) for secure and low-complexity multiple access communications," *RS Open Journal on Innovative Communication Technologies*, vol. 2, no. 4, 6 2021.
- [37] I. S. Gradshteyn and I. M. Ryzhik, *Table of integrals, series, and products*. Academic press, 2014.
- [38] S. Khalid, S. Iqbal, and J. M. Hamamreh, "A new enhanced coordinated multi-point (CoMP) transmission design for cancelling inter-cell interference for cell-edge users using superimposed supporting signals," *RS Open Journal on Innovative Communication Technologies*, vol. 2, no. 6, p. 12, 2021.
- [39] J. M. Hamamreh, M. Abewa, and J. Lemayian, "New non-orthogonal transmission schemes for achieving highly efficient, reliable, and secure multi-user communications," *RS Open Journal on Innovative Communication Technologies*, vol. 1, no. 2, p. 12, 2020.
- [40] S. Iqbal, S. Khalid, and J. M. Hamamreh, "A new MIMO technique utilizing superimposed auxiliary signals for simultaneously achieving spatial multiplexing and diversity gains in MIMO-Aided communication systems," *RS Open Journal on Innovative Communication Technologies*, vol. 2, no. 4, p. 6, 2021.
- [41] J. M. Hamamreh and J. P. Lemayian, "A novel small-scale nonorthogonal communication technique using auxiliary signal superposition with enhanced security for future wireless networks," 2020.
- [42] S. Iqbal, S. Khalid, and J. M. Hamamreh, "Improving the performance of cell-edge users in 6G and beyond networks by utilizing a novel precoding-based hybrid CoMP transmission design."
- [43] M. Abewa and J. M. Hamamreh, "D-SEAD: A novel multi-access multi-dimensional transmission technique for doubling the spectral efficiency per area and per device."
- [44] M. Kirik and J. M. Hamamreh, "Interference signal superposition-aided MIMO with antenna number modulation and adaptive antenna selection for achieving perfect secrecy," *RS Open J. Innov. Commun. Technol*, vol. 2, pp. 1–11, 2021.

- [45] S. Iqbal and J. M. Hamamreh, "Improving throughput and reliability performance of future 6G-IoT communication systems using signal superposition-based dual transmission," *RS Open Journal on Innovative Communication Technologies*, vol. 2, no. 5, p. 9, 2021.
- [46] J. P. Lemayian and J. M. Hamamreh, "Physical layer security analysis of hybrid MIMO technology," *RS Open Journal on Innovative Communication Technologies*, vol. 2, no. 5, p. 8, 2021.
- [47] F. Z. Muhammad, H. M. Furqan, and J. M. Hamamreh, "Multi-cell, multi-user, and multi-carrier secure communication using non-orthogonal signals' superposition with dual-transmission for IoT in 6G and beyond," 2021.
- [48] M. F. Zia and J. M. Hamamreh, "An advanced non-orthogonal multiple access security technique for future wireless communication networks," *RS Open J. Innov. Commun. Technol.*, vol. 1, no. 2, 2020.
- [49] J. M. Hamamreh and H. Arslan, "Joint PHY/MAC layer security design using ARQ with MRC and null-space independent PAPR-aware artificial noise in SISO systems," *IEEE Transactions on Wireless Communications*, vol. 17, no. 9, pp. 6190–6204, 2018.
- [50] J. M. Hamamreh, M. Yusuf, T. Baykas, and H. Arslan, "Cross MAC/PHY layer security design using ARQ with MRC and adaptive modulation," in *2016 IEEE Wireless Communications and Networking Conference*. IEEE, 2016, pp. 1–7.
- [51] J. M. Hamamreh, E. Guvenkaya, T. Baykas, and H. Arslan, "A practical physical-layer security method for precoded OSTBC-based systems," in *2016 IEEE Wireless Communications and Networking Conference*. IEEE, 2016, pp. 1–6.
- [52] M. Kirk and J. M. Hamamreh, "A novel interference signal superposition algorithm for providing secrecy to subcarrier number modulation-based orthogonal frequency division multiplexing systems," *Transactions on Emerging Telecommunications Technologies*, p. e4678, 2022.



SADIQ IQBAL in 2016, obtained his electrical engineering B.E. degree from QUEST University Nawabshah, Pakistan. He is presently pursuing the master's (M.Sc.) degree in electrical and computer engineering. He is currently with Antalya Bilim University, Turkey. His research interests include physical layer technology, 5G communication networks, artificial intelligence, IoT, and its applications.



Jihad M. Hamamreh is the Founder and Director of WISLAB (wislabi.com), and A. Professor at the Electrical and Electronics Engineering Department, Antalya Bilim University. He received his Ph.D. degree in telecommunication engineering and cyber systems from Istanbul Medipol University, Turkey, in 2018. Previously, he worked as a Researcher at the Department of Electrical and Computer Engineering at Texas AM University. He is the inventor of more than 20+ patents and an author of more than 85+ peer-reviewed scientific papers along with several

book chapters. His innovative patented works won gold, silver, and bronze medals at numerous international invention contests and fairs. His current research interests include wireless physical and MAC layer security, orthogonal frequency-division multiplexing and multiple-input multiple-output systems, advanced waveform design, multidimensional modulation techniques, and orthogonal/non-orthogonal multiple access schemes for future wireless systems. He is a serial referee for various scientific journals as well as a TPC member for several international conferences. He is an Editor at Researcherstore, RS-OJICT journal, and Frontiers in Communications and Networks. Email: jihad.hamamreh@gmail.com.